INVERSE RESPONSE OF CHARPY IMPACT AND PLANE STRAIN FRACTURE TOUGHNESS TO MICROSTRUCTURAL VARIATIONS IN A LOW ALLOY STEEL

R. Padmanabhan* and W. E. Wood**

The Charpy impact and plane strain fracture toughness responses of 300M steel were investigated as a function of microstructural variations. CVN energy, in general, dropped with increasing K_{Ic}. However, simultaneous improvement in both these properties was achieved by incorporating a fine grained lath martensite morphology and a fine carbide dispersion through a modified heat treatment process. These results are discussed in terms of the microstructure and fractography analyses.

INTRODUCTION

Utilization of high austenitization temperatures to improve the fracture toughness of UHSLA steels at similar strength levels has received considerable interest (Zackay et al (1), Clark et al (2), Wood et al (3), Lai et al (4) and Zackay et al (5)). In 300M steel, almost two-fold increases in K_{Ic} have been reported (McDarmaid (6) and Youngblood and Raghavan (7)). However, these heat treatments resulted in reduced ductility and impact toughness (Ritchie and Horn (8) and Ferguson et al (9)). The relationships between microstructure, ductility, impact and fracture toughness are examined in this paper. An experimental heat treatment was developed to effect simultaneous increases in both K_{Ic} and CVN energy, by establishing a fine grain size, a lath martensite morphology and a fine dispersion of alloy carbides.

EXPERIMENTAL PROCEDURE

The material used in this investigation was a vacuum remelted 300M steel, whose chemical composition is given in Table 1.

TABLE 1--Chemical Composition of 300M Steel (wt.%)

C	Mn	Si	Cr	Ni	Mo	Cu	S	P	V	Fe
0.42	0.79	1.64	0.79	1.84	0.36	0.05	0.006	0.010	0.08	Balance

* Senior Research Scientist, and ** Chairman and Professor, Department of Materials Science and Engineering, Oregon Graduate Center, Beaverton, Oregon 97006, USA.

The heat treatment schematic is given in Figure 1. All austenitization steps were carried out in a tube furnace under an argon atmosphere and tempering steps in a salt bath furnace, the temperatures being maintained within an accuracy of ±0.3°C. Plane strain fracture toughness was evaluated using 1.6 mm thick compact tension specimens in accordance with ASTM specifications. Tensile properties were determined using 6.35 mm diameter rods at a strain rate of 0.025 cm/min. Charpy V-notch energy was evaluated using 10 mm square Charpy bars with a root radius of 0.25 mm. Thin foil and extraction replica work was carried out using a Hitachi HU-11B transmission electron microscope and fractography studies using a JEOL JSM-35 scanning electron microscope.

RESULTS

The mechanical properties of the various heat treatments are listed in Table 2.

TABLE 2--Mechanical Properties of 300M Steel as a Function of Heat Treatment

Heat Treatment	Prior Austenite Grain Size (μm)	Yield Strength (MNm^{-2})	Ultimate Tensile Strength (MNm^{-2})	Elongation (%)	Reduction in Area (%)	CVN Energy (Nm)	Plane Strain Fracture Toughness ($MNm^{-3/2}$)
Conventional	20	1621.0	1963.0	11.1	39.5	27.1	55.9
High Temperature	220	1656.2	2002.3	5.8	11.7	17.7	91.2
Step	220	1493.9	1818.0	8.5	16.1	12.4	78.9
Modified Conventional	15	1730.9	1978.2	13.8	46.7	27.2	101.5

High temperature and step heat treatments improved K_{Ic} by about 35$MNm^{-3/2}$ and 23 $MNm^{-3/2}$, respectively, over the conventional heat treatment,while the CVN energy decreased by about 9.5 Nm and 15 Nm, respectively. The yield strength remained almost identical for the high temperature and conventional heat treatment, but was lowered by about 127 MNm^{-2} for the step heat treatment. The high temperature and step heat treatments also resulted in significantly lower elongation and reduction in area. The modified conventional heat treatment improved K_{Ic} by about 45 $MNm^{-3/2}$ and yield strength by about 110 MNm^{-2} over the conventional heat treatment. While the ductility values were also slightly higher, CVN energy and yield strength remained essentially unchanged.

The fracture modes of the various K_{Ic} specimens are compared in Figure 2. All heat treatments resulted in predominantly microvoid coalescence failure in the initiation region, with conventional, high temperature and step heat treatments exhibiting some intergranular and quasi-cleavage failure. Dimple size was smallest for modified conventional heat treatment and largest for high temperature and step heat treatments, with conventional heat treatment possessing an intermediate value. CVN and tensile specimens also exhibited microvoid coalescence failure in the fracture initiation region.

Bright field pictures typifying the general structure are presented in Figure 3. All heat treatments remelted in a mixture of lath and plate martensite, with twinned plate martensite predominating for the conventional heat treatment. The average lath width was about 0.3μ for conventional, high

temperature and step heat treatments and about 0.25μ for modified conventional heat treatment. The tendency for twinning decreased for step, high temperature and modified conventional heat treatments, in the same order. ε-carbide and cementite were the predominating carbide types. However, in the case of the modified conventional heat treatment, finely dispersed alloy carbides of the types M_3C, M_7C_3, Mo_2C, and $M_{23}C_6$ were also identified. From dark field imaging using $(002)_\gamma$ and $(111)_\gamma$ spots, the amount of retained austenite was estimated to be about 6 to 8% for the high temperature, step, and modified conventional heat treatments and about 3% for the conventional heat treatment.

DISCUSSION

CVN energy consistently dropped with an increase in K_{Ic}. While the notch root radius tends to zero for the K_{Ic} specimens, it is 0.25 mm for CVN specimens. The anamolous toughness behavior is explained based on this notch root radius variation.

Fractography results showed that the predominant failure mode for all the heat treatments was microvoid coalescence. For strain controlled fracture, a model has been proposed in which the extensional strain, ε, must exceed the critical fracture strain ε_f (Ritchie (10)). The apparent fracture toughness K_A can then be expressed as

$$K_A \simeq (3/2\ \sigma_{ys}\ E\ \varepsilon_f)^{1/2}\ \rho^{1/2} \qquad (1)$$

According to this model, below a certain critical radius ρ_o, K_A becomes independent of ρ and has the same value as K_{Ic}, and, hence,

$$K_{Ic} \simeq (3/2\ \sigma_{ys}\ E\ \varepsilon_f)^{1/2}\ \rho_o^{1/2} \qquad (2)$$

ρ_o is the measure of a characteristic distance over which the critical strain is exceeded for failure. For microvoid coalescence failure, this distance is proportional to the interparticle spacing.

The variation of CVN energy with ductility is consistent with the predictions in equation (1). Conventional and modified conventional heat treatments with high ductility values also resulted in high CVN energy values. Equation (2) predicts an increase in K_{Ic} with an increase in interparticle spacing (dimple size). While this is observed for conventional, high temperature and step heat treatments, the modified conventional heat treatment with the smallest interparticle spacing (smallest ρ_o) still yielded the highest K_{Ic} value. This is attributable to the elevation of critical fracture strain due to other microstructural effects.

Retained austenite, if stable, can improve fracture toughness (Antolovich et al (11) and Webster (12)). For high temperature, step and modified conventional heat treatments, almost twice the amount of retained austenite was observed when compared with the conventional heat treatment. Retained austenite, observed in this study, was thermally stable. While its mechanical stability was not investigated, transformation of this retained austenite (if unstable) to martensite would absorb about five times more energy than for the plastic deformation of a stable metal matrix (Gerberich and Birat (13)).

Extensive twinning was observed in the conventional heat treatment. Twins lower fracture toughness and increase strength (Maki et al (14) and

Kelly and Nutting (15)). Although the twin density variation is consistent with the K_{Ic} variation for these heat treatments, other significant factors which govern K_{Ic} are the lath width and packet size. In all the heat treatments, lath martensite morphology was observed. The fracture stress in such a matrix can be written as (Naylor (16)):

$$\sigma_f = \left[\frac{1.4LE\gamma_1'}{n\, d_p\, \varepsilon_1}\right]^{1/2} \qquad (3)$$

Decreasing lath width and packet diameter combine to elevate σ_f (and, hence, ε_f) and thus K_{Ic}. The packet diameter was highest for high temperature and step heat treatments and lowest for modified conventional heat treatment. The average lath width was also smallest for the latter heat treatment. Thus, K_{Ic} of the latter heat treatment exhibits the maximum increase.

Summarizing, CVN energy varied in accordance with ductility variations. K_{Ic} varied not only as a function of interparticle spacing but also as a function of other microstructural variables (both as a function of critical root radius and fracture strain).

CONCLUSIONS

CVN energy generally varied as an inverse function of K_{Ic} and grain size and as a direct function of ductility, for strain controlled fracture. From toughness analysis, a larger interparticle spacing, increased retained austenite, reduced twin density and smaller lath width and packet diameter all raise ε_f and increase K_{Ic}. A concurrent increase in CVN energy and K_{Ic} was achieved by controlled variations in the microstructure, which decreased grain size while increasing ε_f.

SYMBOLS USED

CVN energy = Charpy V-notch energy (Nm)

K_{Ic} = plane strain fracture toughness ($MNm^{-3/2}$)

UHSLA Steels = ultrahigh strength low alloy steels

ε = extensional strain (mm/mm)

ε_f = critical fracture strain (mm/mm)

K_A = apparent fracture toughness ($MNm^{-3/2}$)

σ_{ys} = yield strength (MNm^{-2})

E = elasticity modulus (MNm^{-2})

ρ = notch root radius (mm)

ρ_o = critical notch root radius (mm)

σ_f = critical fracture stress (MNm^{-2})

L = critical length of the crack (mm)

γ_1' = energy needed to achieve deviations across "n" laths

d_p = packet diameter (μm)

ε_1 = lath width (μm)

REFERENCES

1. Zackay, V. F., Parker, E. R., Goolsby, R. D., and Wood, W. E., 1972, Nat. Phy. Sci., 236, 108.
2. Clark, R. A., Ritchie, R. O., and Knott, J. F., 1972, Nat. Phy. Sci., 239, 104.
3. Wood, W. E., Parker, E. R., and Zackay, V. F., 1973, LBL Report #1474.
4. Lai, G. Y., Wood, W. E., Clark, R. A., Zackay, V. F., and Parker, E. R., 1974, Met. Trans., 5A, 1663.
5. Zackay, V. F., Parker, E. R., and Wood, W. E., 1974, The Met. Soc. (Lon.), 1, 175.
6. McDarmaid, D. S., 1978, Met. Tech., 5, 7.
7. Youngblood, J. L., and Raghavan, M. R., 1977, Met. Trans., 8A, 1439.
8. Ritchie, R. O., and Horn, R. M., 1978, Met. Trans., 9A, 331.
9. Ferguson, W. G., Clark, N. E., and Watson, B. R., 1976, Met. Tech., 3, 208.
10. Ritchie, R. O., 1978, Proc. Ann. Meeting of the Amer. Inst. of Mining, Metallurgical and Petroleum Engineers, 54.
11. Antolovich, S. D., Saxena, A., and Chanani, G. R., 1974, Met. Trans., 5A, 623.
12. Webster, D., 1971, Met. Trans., 2A, 2097.
13. Gerberich, W. W., and Birat, J. P., 1971, Int. J. of Fr. Mech., 7, 108.
14. Maki, T., Shimooka, S., Umemoto, M., and Tamura, I., 1971, Met. Trans., 2A, 2944.
15. Kelly, P. M., and Nutting, J., 1961, JISI, 199.
16. Naylor, J. P., 1979, Met. Trans., 10A, 861

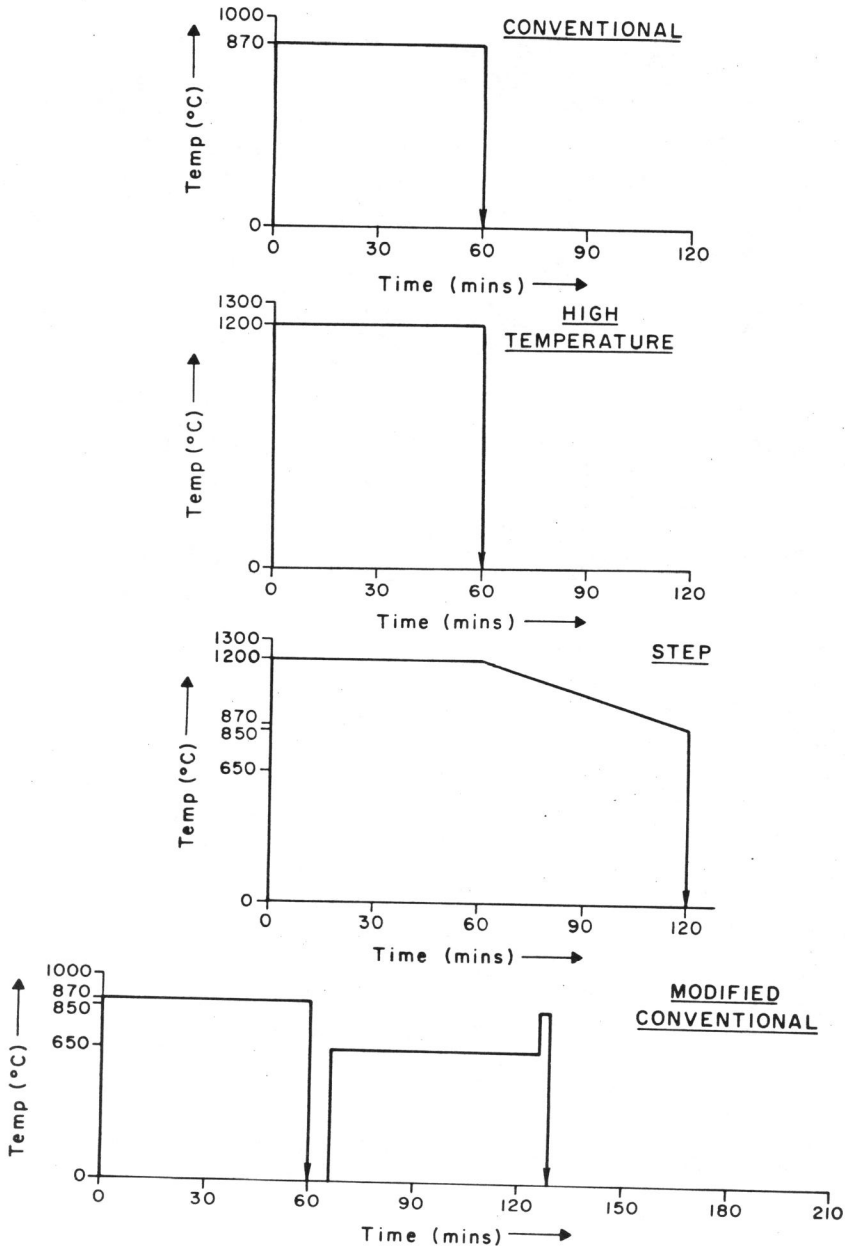

Figure 1 Heat treatment schematic

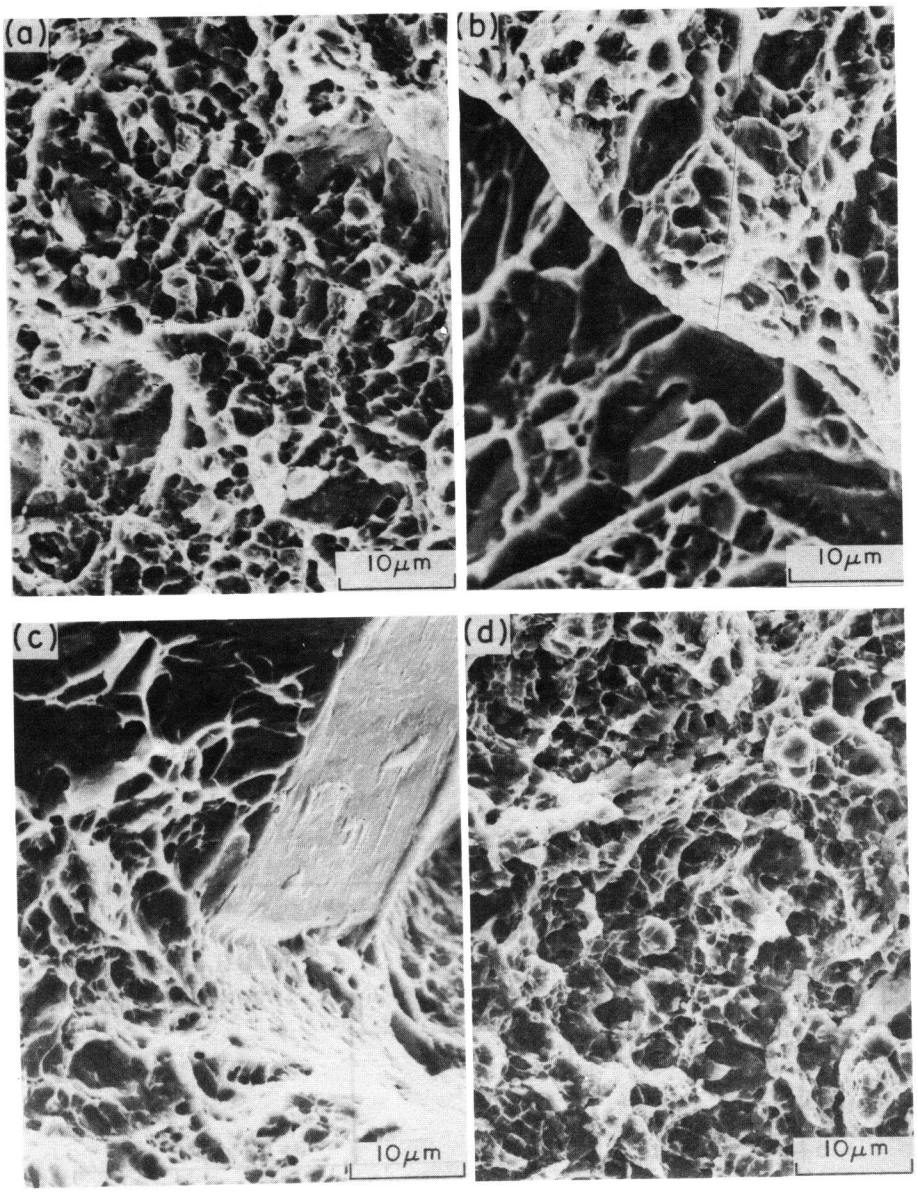

Figure 2 S.E.M. fractographs of K_{Ic} specimens revealing the initiation region failure modes: a) conventional, b) high temperature, c) step, and d) modified conventional heat treatments, 2000x

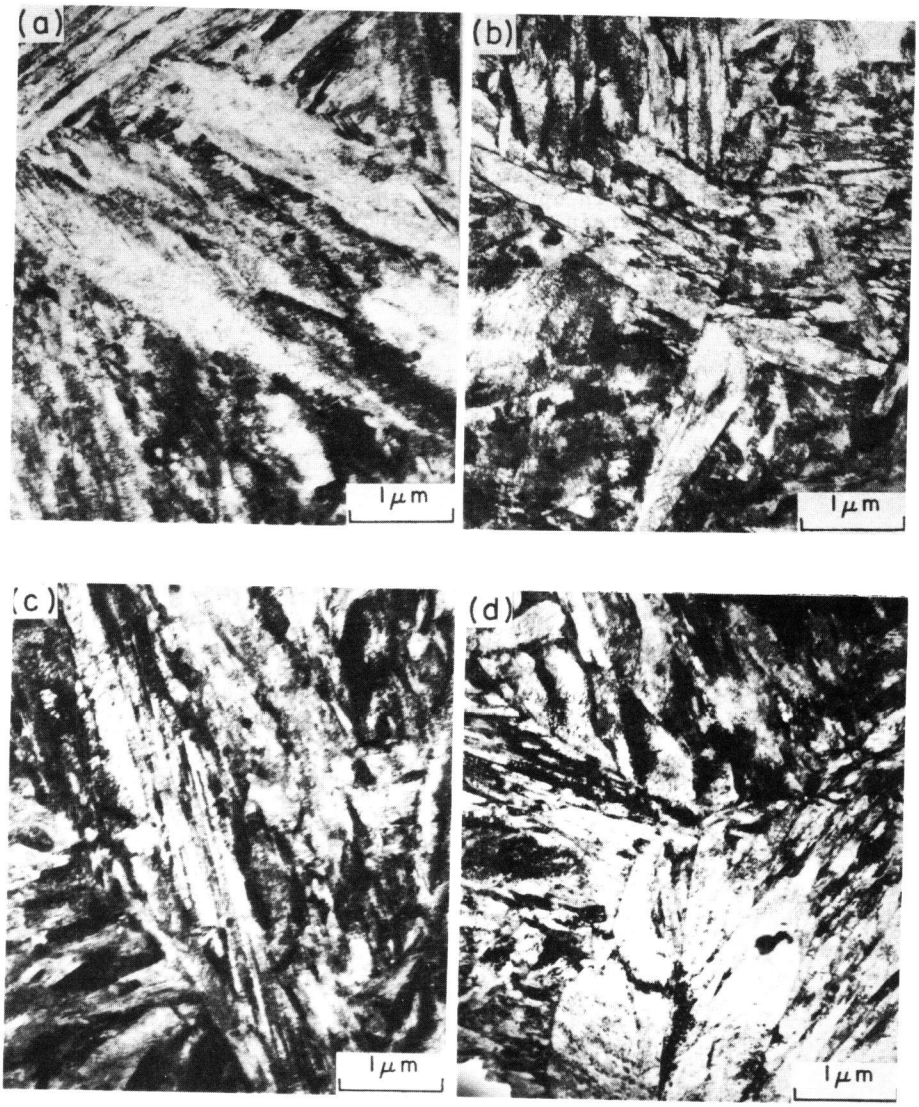

Figure 3 T.E.M. bright field micrographs indicating the martensite substructure: a) conventional, b) high temperature, c) step, and d) modified conventional heat treatments, 18600x